Bioorganic & Medicinal Chemistry 17 (2009) 1361–1369

Contents lists available at ScienceDirect

Bioorganic & Medicinal Chemistry

journal homepage: www.elsevier.com/locate/bmc

Isolation, structure and biological activity of phomafungin, a cyclic lipodepsipeptide from a widespread tropical *Phoma* sp.

Kithsiri Herath [a], Guy Harris [a], Hiranthi Jayasuriya [a], Deborah Zink [a], Scott Smith [a], Francisca Vicente [b], Gerald Bills [b], Javier Collado [b], Antonio González [b], Bo Jiang [c], Jennifer Nielsen Kahn [d], Stefan Galuska [d], Robert Giacobbe [d], George Abruzzo [d], Emily Hickey [d], Paul Liberator [d], Deming Xu [c,*], Terry Roemer [c,d], Sheo B. Singh [a,*]

[a] *Natural Products Chemistry, Merck Research Laboratories, Rahway, NJ 07065, USA*
[b] *Centro de Investigación Básica, Merck Sharp & Dohme de España, S. A., Madrid, Spain*
[c] *Center of Fungal Genetics, Merck Frosst Canada Ltd., Montreal, Quebec, Canada*
[d] *Infectious Disease, Merck Research Laboratories, Rahway, NJ 07065, USA*

ARTICLE INFO

Article history:
Received 29 September 2008
Revised 4 December 2008
Accepted 7 December 2008
Available online 14 December 2008

Keywords:
Natural product
Antifungal agent
Cyclic depsipeptide
Candida albicans fitness test (CaFT)
Genome-wide target based screening

ABSTRACT

We isolated a cyclic lipodepsipeptide, phomafungin, from a *Phoma* sp. The distinct antifungal activity of phomafungin in the crude extract was initially discovered by mechanistic profiling in the *Candida albicans* fitness test. The purified compound contains a 28 member ring consisting of eight amino acids and a β-hydroxy-γ-methyl-hexadecanoic acid, and displays a broad spectrum of antifungal activity against *Candida* spp., *Aspergillus fumigatus* and *Trichophyton mentagrophytes* with MIC of 2–8 μg/ml, and toxicity to mice at 25 mg/kg. The linear peptide derived from opening of the lactone ring was devoid of antifungal activity as well as toxicity. Phomafungin has been identified in a number of *Phoma* spp. collected from Africa and the Indian and Pacific Ocean islands.

© 2009 Elsevier Ltd. All rights reserved.

1. Introduction

Candida albicans (and other species) and filamentous pathogens (*Aspergillus fumigatus*, in particular) pose a serious threat to immunocompromised patients in the hospital setting.[1] Current treatments of fungal infections are limited to amphotericin B,[2] azoles[3] and echinocandins,[4] with acceptable results. However, the changing epidemiology and emergence of resistant strains call for new antifungal drugs with broad spectra and distinct mechanisms of action. We maintain that natural products remain the most prolific repertoire of compounds with diverse structures, and likely diverse bioactivities. But the traditional 'grind-and-find' approach, including bioassay-guided isolation based on conventional whole-cell screening approaches, has been seriously challenged by the frequent rediscovery of known compounds. To circumvent this problem, we have implemented new approaches that enhance the biodiversity of natural products,[5] and dereplicate and cluster the natural products according to their bioactivities.[6–8] In this way, only extracts with distinct bioactivities, likely new chemical structures, are selected for fractionation.

The *C. albicans* fitness test (CaFT) takes advantage of the diploidy of the pathogen that changes growth of heterozygous deletion strains in the presence of antiproliferative agents. As demonstrated, most target- or mechanism-specific antifungal compounds induce hyper- and hypo-sensitivity only in heterozygous deletion strains that are indicative of the targets and aspects of mechanisms of action.[8] Conversely, an informative CaFT profile of a synthetic compound or a natural product may shed mechanistic light on the biological activity. Applied directly to crude extracts (e.g., microbial fermentation broth), mechanistic profiling using the fitness test provides a biological solution to dereplication of natural products. Extracts with distinct CaFT profiles are likely to contain distinct biological activities, which are likely attributable to distinct chemical entities. Since the heterozygous deletion strains employed in the CaFT cover approximately 45% of the pathogen genome, mechanistic dereplication is an inclusive approach that overcomes the limitation of target-based screening. Our strategy has been validated by the discovery of parnafungins from a fungal source that are novel and potent inhibitors of RNA poly(A) polymerase with a broad

* Corresponding authors. Tel.: +1 732 594 3222; fax: +1 732 594 6880 (S.B. Singh).
E-mail addresses: xu_deming@hotmail.com (D. Xu), sheo_singh@merck.com (S.B. Singh).

0968-0896/$ - see front matter © 2009 Elsevier Ltd. All rights reserved.
doi:10.1016/j.bmc.2008.12.009

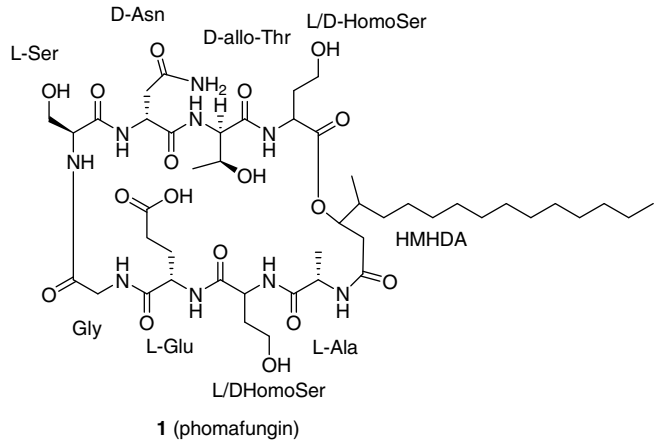

Figure 1. Chemical structure of phomafungin isolated from *Phoma* spp.

antifungal spectrum and in vivo efficacy against a murine model of candidiasis,[9,10]

Here we report the identification, isolation and characterization of a cyclic lipodepsipeptide, phomafungin (**1**, Fig. 1), produced by a widespread tropical *Phoma* spp. The original extract produced a complex profile in the CaFT indicative for genes involved in the sphingolipid biosynthesis. However, the profile was distinct from those of known sphingolipid inhibitors previously tested in CaFT. Analytical HRLCMS indicated that the extract did not contain known inhibitors of fungal sphingolipid pathway. Bioassay-guided isolation led to phomafungin (**1**), which reproduced the original profile in the CaFT, and displays a broad antifungal activity against *Candida spp.* and other human fungal pathogens.

2. Results and discussion

2.1. Identification of phomafungin-containing extracts in the CaFT

To enhance the diversity of secondary metabolites, terrestrial fungal isolates were grown in eight-nutrient medium micro fermentation arrays. Once whole-cell antifungal activity was detected for a particular strain, fermentation was scaled up to one liter under the optimal conditions. The mycelium and fermentation broth were extracted with acetone and tested in the CaFT. The extract of strain F-224,939 produced a complex profile characterized by four hypersensitive heterozygotes corresponding to genes involved in the sphingolipid biosynthesis (*LCB2*, *RTA2*/*RSB1*, *MIT1*/*SUR1*/*CSH1*, and *AUR1*), and those involved in the control of Ca^{2+}, *CMD1* (calmodulin), *orf19.4726*/*FRQ1* (Ca^{2+} binding) and *PMC1* (Ca^{2+}-ATPase), with the last two being hyposensitive. Additional hyper- and hypo-sensitive strains did not indicate any particular cellular process(es) being specifically affected by this extract (Fig. 2). However, compared with known inhibitors of sphingolipid (myriocin,[11] aureobasidin A[12,13] and rustimicin[14,15]), the largely non-overlapping profile of F-224,939 (Fig. 2) indicated the presence of a distinct biological activity. Analytical HRLCMS failed to identify myriocin,[11] rustimicin,[14,15] minimoidin,[16] aureobasidins,[13,17] australifungin,[15] and syringomycins[18] in this extract (data not shown). The producing fungus was identified as a *Phoma* sp. based on microscopic morphology and ITS and 28S rDNA sequences (see below).

2.2. Isolation and structural elucidation of phomafungin

Extract of F-224,939 was chromatographed on Amberchrome reversed-phase column eluted with a 5–100% aqueous methanol linear gradient. Liquid–liquid partition of the fractions with antifungal activity followed by reversed-phase HPLC led to purified phomafungin (156 mg/L) as an amorphous powder. The purified phomafungin (**1**, Fig. 1) produced a CaFT profile consistent with the original (Fig. 2), suggesting that the biological activity detected in the CaFT could be attributed solely to phomafungin.

Mass spectral analysis of **1** provided a molecular weight of 1029 and a formula of $C_{46}H_{79}N_9O_{17}$. The UV spectrum showed an end absorption, and the IR spectrum displayed the presence of hydroxy and carbonyl groups. The ^{13}C NMR spectrum in DMSO-d_6 showed the presence of 40 distinct resonances and six degenerate resonances. The spectral data revealed the presence of 11 carboxyl carbonyls along with a large number of signals resonating in the methylene region of the spectrum, indicating that the compound was a lipopeptide. This data along with DEPT spectrum suggested the presence of 7 α-methines, 2 oxymethines, an aliphatic methine, 3 oxymethylenes, 18 methylenes, and 4 methyls (Table 1). The ^1H NMR together with COSY, TOCSY and HSQC spectral data provided evidence for the presence of an alanine, a glycine, a serine, 2 homoserines, a threonine, a glutamic acid (or glutamine), and an asparagine (or aspartic acid). It was clear from the NMR spectrum that the remaining moiety contained a β-hydroxy-γ-methyl fatty acid (Table 1) which was elucidated as β-hydroxy-γ-methyl-hexadecanoic acid (HMHDA) by subtraction of the amino acid units from the formula. The sequencing of the peptide was performed first by HMBC correlations of the amide NH's and α-protons to corresponding amide carbonyls of the cyclic depsipeptide and was corroborated by ESI MS–MS analysis of the hydrolyzed product.

Basic hydrolysis of compound **1** produced the linear peptide **2** which showed a protonated molecular ion at *m/z* 1048. The fragmentation pattern of the linear peptide is shown in Figure 3. The fragmentation produced both *b* and *y″* type fragment ions *m/z* 929, 828, 714, 627, 570, 441, and 340 due to sequential losses of Homoser, Thr, Asn, Ser, Gly, Glu and Homoser thus suggesting a sequence as Homoser-Thr-Asn-Ser-Gly-Glu-Homoser-Ala-HMHDA. Clearly, the mass spectral data did not distinguish between Thr and homoserines. The complete sequence was confirmed by HMBC correlations of α-proton and α-NH protons to the corresponding carboxyl carbonyls and α-carbons of the cyclic peptide in DMSO-d_6 (Fig. 4). For example, α-proton (H-2) of homoser-1 showed HMBC correlations to the homoser-1 carbonyl and its α-NH

Figure 2. CaFT profiles of myriocin, aureobasidin A (AbA), rustimicin, phomafungin and the fermentation extracts of *Phoma* spp. Three independent CaFT experiments, with different inhibitory concentrations (ICs), were selected for each reference compounds. The relative behavior of each heterozygous deletion strain elicited by antiproliferative agents in each experiment is expressed statistically by two normalized *z*-scores, corresponding to two DNA barcodes introduced at the deleted allele, with positive value indicating hypersensitivity, and negative resistance. For each strain in a particular experiment, the *z*-score of higher absolute value was selected.[8] To compare the CaFT profiles, strains with absolute value of *z*-scores no less than 3 in at least three experiments were selected. They (93 in total from the experiments chosen) were grouped by hierarchical clustering using centroid linkage method,[36] the result of which is displayed in TreeView with *z*-scores between +1.5 and −1.5 masked, with scale of the heat map shown in the top-right corner, and, the hierarchical linkage on the top, together with the identities of antifungal actives and experimental conditions. The heterozygous deletion strains are indicated by the orf19 designations of the corresponding genes, with *C. albicans* genes and *S. cerevisiae* orthologs/homologs (if any) indicated on the right of the heat map. The *C. albicans* genome annotation is adapted from the *Candida* Genome Database (www.candidagenome.org). Highlighted in red are those involved in sphingolipid biosynthesis, in blue Ca^{2+} regulation (see text for detail).

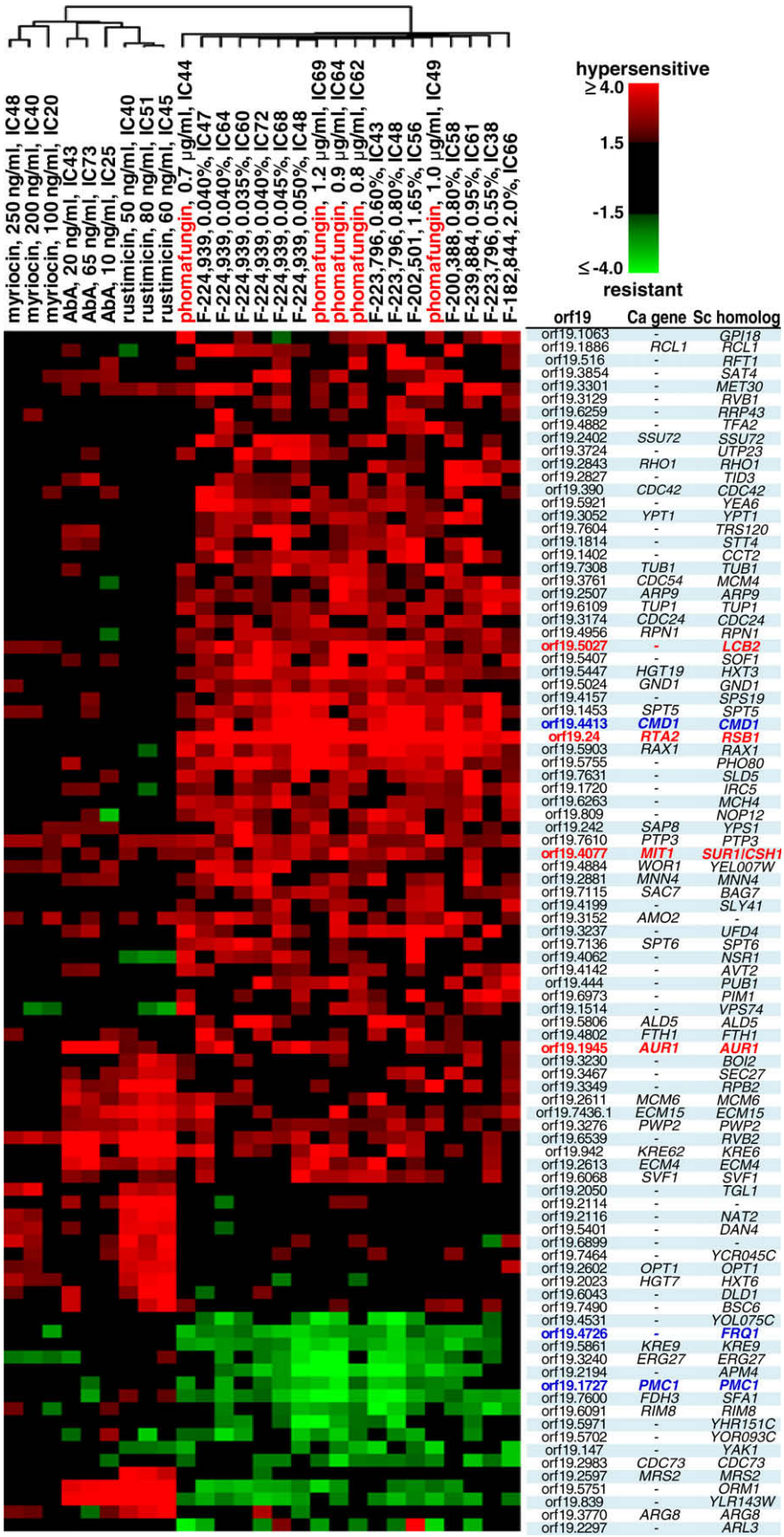

orf19	Ca gene	Sc homolog
orf19.1063	-	GPI18
orf19.1886	RCL1	RCL1
orf19.516	-	RFT1
orf19.3854	-	SAT4
orf19.3301	-	MET30
orf19.3129	-	RVB1
orf19.6259	-	RRP43
orf19.4882	-	TFA2
orf19.2402	SSU72	SSU72
orf19.3724	-	UTP23
orf19.2843	RHO1	RHO1
orf19.2827	-	TID3
orf19.390	CDC42	CDC42
orf19.5921	-	YEA6
orf19.3052	YPT1	YPT1
orf19.7604	-	TRS120
orf19.1814	-	STT4
orf19.1402	-	CCT2
orf19.7308	TUB1	TUB1
orf19.3761	CDC54	MCM4
orf19.2507	ARP9	ARP9
orf19.6109	TUP1	TUP1
orf19.3174	CDC24	CDC24
orf19.4956	RPN1	RPN1
orf19.5027	**-**	**LCB2**
orf19.5407	-	SOF1
orf19.5447	HGT19	HXT3
orf19.5024	GND1	GND1
orf19.4157	-	SPS19
orf19.1453	SPT5	SPT5
orf19.4413	**CMD1**	**CMD1**
orf19.24	**RTA2**	**RSB1**
orf19.5903	RAX1	RAX1
orf19.5755	-	PHO80
orf19.7631	-	SLD5
orf19.1720	-	IRC5
orf19.6263	-	MCH4
orf19.809	-	NOP12
orf19.242	SAP8	YPS1
orf19.7610	PTP3	PTP3
orf19.4077	**MIT1**	**SUR1/CSH1**
orf19.4884	WOR1	YEL007W
orf19.2881	MNN4	MNN4
orf19.7115	SAC7	BAG7
orf19.4199	-	SLY41
orf19.3152	AMO2	-
orf19.3237	-	UFD4
orf19.7136	SPT6	SPT6
orf19.4062	-	NSR1
orf19.4142	-	AVT2
orf19.444	-	PUB1
orf19.6973	-	PIM1
orf19.1514	-	VPS74
orf19.5806	ALD5	ALD5
orf19.4802	FTH1	FTH1
orf19.1945	**AUR1**	**AUR1**
orf19.3230	-	BOI2
orf19.3467	-	SEC27
orf19.3349	-	RPB2
orf19.2611	MCM6	MCM6
orf19.7436.1	ECM15	ECM15
orf19.3276	PWP2	PWP2
orf19.6539	-	RVB2
orf19.942	KRE62	KRE6
orf19.2613	ECM4	ECM4
orf19.6068	SVF1	SVF1
orf19.2050	-	TGL1
orf19.2114	-	-
orf19.2116	-	NAT2
orf19.5401	-	DAN4
orf19.6899	-	-
orf19.7464	-	YCR045C
orf19.2602	OPT1	OPT1
orf19.2023	HGT7	HXT6
orf19.6043	-	DLD1
orf19.7490	-	BSC6
orf19.4531	-	YOL075C
orf19.4726	**-**	**FRQ1**
orf19.5861	KRE9	KRE9
orf19.3240	ERG27	ERG27
orf19.2194	-	APM4
orf19.1727	**PMC1**	**PMC1**
orf19.7600	FDH3	SFA1
orf19.6091	RIM8	RIM8
orf19.5971	-	YHR151C
orf19.5702	-	YOR093C
orf19.147	-	YAK1
orf19.2983	CDC73	CDC73
orf19.2597	MRS2	MRS2
orf19.5751	-	ORM1
orf19.839	-	YLR143W
orf19.3770	ARG8	ARG8
orf19.2297	-	ARL3

Table 1
^{1}H, ^{13}C and ^{15}N NMR assignments of phomafungin (38.9 μM) in DMSO-d_6

AA	Position	Mult	δ_C (δ_N)	δ_H, mult, J in Hz	HMBC (H→C,N)	Key NOESY[a]
L/D Homoser1 (HS1)	1	CO	171.2			
	2	CH	49.9	4.27, ddd, 8.4, 7.2, 4.8	C-1, 3, 4, α-N, Thr (C-1)	
	3	CH_2	34.0	1.76, m 1.82, m	C-1, α-N	
	4	CH_2	57.0	3.41, m 3.38, m	C-2	
	α-NH		(122.0)	8.2, d, 7.0	C-2, Thr (C-1)	H-3, 4, AT (H-2, 3, 4, NH)
	OH			4.58, t, 4.8	C-3, 4	
D-Allo-Thr (AT)	1	CO	169.9			
	2	CH	58.1	4.20, m	C-2, 3	
	3	CH	67.1	3.88, m	C-1, 2, 4	
	4	CH_3	19.4	1.05, d, 6.6	C-2, 3	
	NH		(114.5)	7.42, d, 7.8	C-2, Asn (C-1)	H-3, 4, Asn (H-2, 3, NH)
	OH			4.90, d, 4.8	C-2, 3, 4	
D-Asn	1	CO	170.4			
	2	CH	50.0	4.47, br q, 7.2	C-1, 2, 3	
	3	CH_2		2.43, dd, 15.6, 6.6 2.63, dd, 15.6, 6.6	C-1, 2, 4, α-N	
	4	CO				
	NH		(120.5)	8.16, d, 7.8	C-2, 3, Ser (C-1)	H-3, Ser (H-2, 3), AT (H-3 w, NH)
	NH_2		(112.5)	6.88, brs 7.36, brs	C-3, 4 C-3, 4	
L-Ser	1	CO	170.0			
	2	CH	55.7	4.21, m	C-3, α-N	
	3	CH_2	61.3	3.54, m	C-1, 2, α-N	
	NH		(117)	8.05, d, 5	C-2, Gly (C-1)	H-3, Gly (H-2)
Gly	1	CO	169.3			
	2	CH_2	42.3	3.92, dd, 16.6, 6.6 3.51, dd, 16.6, 5.4	C-1, Glu (C-1), α-N	
	NH			7.98, brt, 5.4	C-2, Glu (C-1)	Glu (H-2, 3, 4)
L-Glu	1	CO	171.6			
	2	CH	51.9	4.20, m	C-1, 3, 4	
	3	CH_2	26.4	1.97, m 1.73, m	C-1, 2, 4, 5	
	4	CH_2	29.8	2.17, m	C-2, 3, 5	
	5	CO	173.8			
	NH		(116.5)	7.86, d, 7.2	C-2, HS2 (C-1)	H-3, 4, HS2 (H-2, 3, 4)
L/D-Homoser2 (HS2)	1	CO	172.2			
	2	CH	51.4	4.15, dt, 8.0, 6.0	C-1, 3, 4	
	3	CH_2	34.0	1.76, m 1.81, m	C-1, α-N	
	4	CH_2	57.5	3.46, m 3.41, m	C-2	
	NH		(118.5)	7.92, d, 6.0	C-2, 3, Ala (C-1)	H-3, 4, Ala (H-2, 3), HA (H-3 w)
	OH			4.55, brs	C-3, 4	
L-Ala	1	CO	172.9			
	2	CH	48.8	4.20, m	C-1, 3, α-N	
	3	CH_3	17.4	1.21, d, 6.6	C-1, 2, α-N	
	NH		(128)	7.82, d, 6.6	C-2, HA (C-1)	H-3, HA (H-2, H-3, 5)
HMHDA (HA)	1	CO	169.8			
	2	CH_2	37.1	2.21, dd, 14.4, 1.8 2.31, dd, 14.4, 10.2	C-1, 3, 4	
	3	CH	75.1	5.01, ddd, 9.6, 4.8, 1.8	C-1, 17, 4, 5, HS2 (C-1)	H-5, 17
	4	CH	36.1	1.61, m	C-3, 5, 6, 17	
	5	CH_2	31.6	1.04, m 1.27, m	C-3, 4, 6, 7	
	6	CH_2	26.4	1.21, m		
	7	CH_2	29.0	1.21, m		
	8–13	CH_2	29.2–28.7	1.21, m		
	14	CH_2	31.3	1.21, m		
	15	CH_2	22.1	1.21, m		
	16	CH_3	13.9	0.83, t, 6.6	C-14, 15	
	17	CH_3	14.5	0.79, d, 6.6	C-3, 4, 5	

[a] Mixing time 300 ms, vicinal and geminal correlations are not listed.

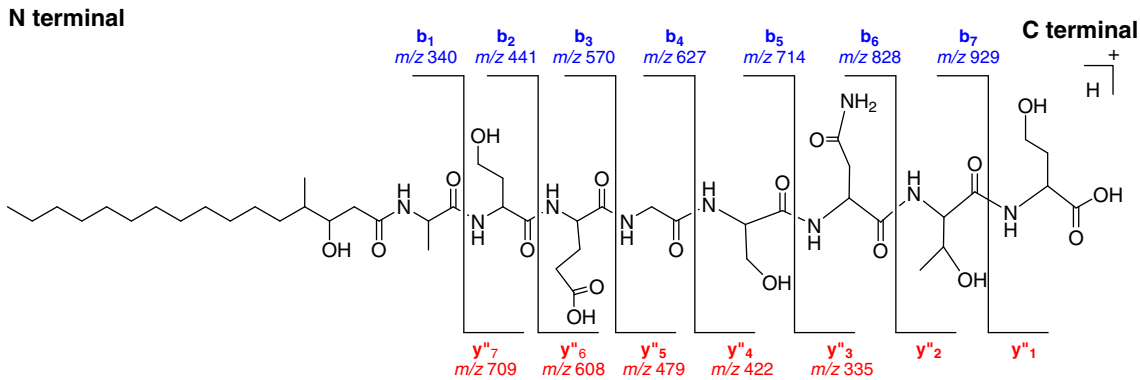

Figure 3. MS/MS fragmentation of linear peptide (**2**) derived from basic hydrolysis of (**1**).

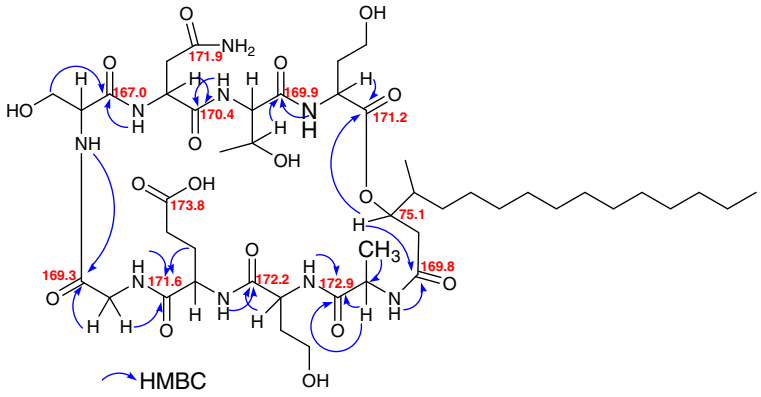

Figure 4. Key HMBC correlations establishing cyclodepsipeptide sequence.

showed HMBC correlations to the carboxyl carbonyl of the adjacent Thr moiety thus confirming the amide bond between the two amino acids. Similar correlations of the α-proton and α-NH confirmed the amide bonds between the remaining amino acids. The HMBC correlations of the β-proton (H-3) of HMHDA showed HMBC correlations to the C-1 of homoser-1 and the C-1 of the HMHDA. The latter carboxyl carbonyl also showed HMBC correlation to Ala α-NH thus confirming the amide bond between Ala and HMHDA and the lactone ring between homoser-1 and HMHDA. The NH assignment was made by ^{1}H, ^{15}N-HSQC experiment which showed 9 well resolved cross peaks for 8 NH and an NH_2 groups. The ^{1}H, ^{15}N-HMBC correlations further corroborated the peptide sequence (Table 1).

The presence of individual amino acids and their absolute configuration was determined by preparation of Marfey's derivatives of the acid hydrolyzed product and HPLC comparison with the derivatives of the corresponding amino acid standards. This method confirmed the presence of one unit each of D-allo-Thr, D-Asn, L-Ser, L-Glu, L-Ala, L-Homoser and D-Homoser. The presence of one unit each of the D- and L-homoser did not allow the confirmation of the specific location of the D- or L-homoser. This could be elucidated by partial hydrolysis and similar analysis of the fragments. However attempts to the partial hydrolysis were unsuccessful due to the lack of specific hydrolytic cleavages providing distinct fragments that could allow this differentiation. The absolute configuration of HMHDA was not determined at this point. Based on the combination of the data a cyclo-{HMHDA-L-Ala-Homoser-L-Glu-Gly-L-Ser-D-Asn-D-allo-Thr-Homoser} depsipeptide structure **1** was established for phomafungin.

Table 2
Effect of 70 °C (25–105 °C) temperature gradient on differential ^{1}H NMR chemical shifts and temperature coefficient of phomafungin 38.9 mM in DMSO-d_6

Protons	$\Delta\delta$ ($\delta_{105}-\delta_{25}$) ppm	Temperature coefficient[a]
HS1-NH	−0.39	−4.9
Asn-NH	−0.29	−3.6
Asn-NH_2	−0.20	−4.0
Asn-NH_2	−0.21	−4.2
Ser-NH	−0.40	−5.0
Gly-NH	−0.22	−2.8
HS2-NH	−0.17	−2.1
Glu-NH	−0.15	−1.9
Ala-NH	−0.28	−3.5
AT-NH	−0.01	−0.1
HOD	−0.37	−4.6
AT-CH_3	0.05	0.6

[a] Temperature coefficient ($\Delta\delta/\Delta T \times 1000$) ppb/°C.

NOESY correlations (Table 1) confirmed the sequence and the assignment of structure but did not provide insight for the configurational assignments of unassigned centers due to significant molecular flexibility which was corroborated by the measurement of chemical shifts of amide protons at temperature gradient. The ^{1}H NMR spectra of 38.9 mM phomafungin in DMSO-d_6 was recorded at 10 °C intervals starting with 25 °C and ending at

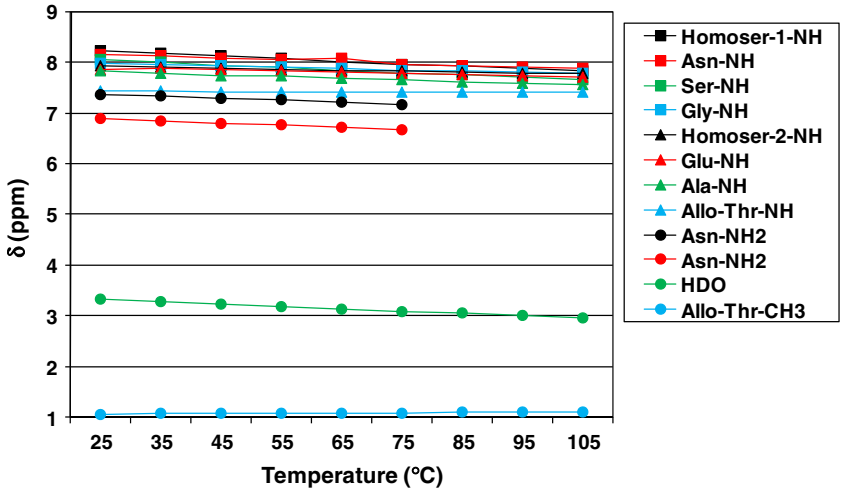

Figure 5. ^{1}H NMR chemical shifts of amide protons of phomafungin (38.9 mM) recorded at 10 °C intervals from 25 °C to 105 °C ($\Delta\delta/\Delta T$ = 80 °C) in DMSO-d_6.

105 °C. The chemical shifts of all amide protons are plotted against temperature (Fig. 5). The slope of the curve ($\Delta\delta$) and temperature coefficient ($\Delta\delta/\Delta T$ in ppb/°C)[19–21] of these and a number of other selected protons are tabulated in Table 2. For internal comparison the chemical shift differences of residual water (HDO) and threonine methyl group is included in Table 2 and in Fig. 5. The chemical shift of the HDO is expected to show largest effect caused by temperature gradient resulting in largest temperature coefficient value. Similarly amide protons that show temperature coefficient values similar to HDO would not be expected to show intra-molecular H-bonding.[22] Comparison of the temperature coefficients of the amide protons indicate that most of the temperature coefficient values are similar to those of HDO suggesting the lack of intra-molecular H-bonding. The only exception was the chemical shift of threonine amide NH which exhibited temperature coefficient of −0.1 ppb/°C similar to the chemical shift of threonine methyl group (0.6 ppb/°C). The threonine amide NH likely makes a strong seven center H-bond with the C-4 carboxy amide carbonyl of Asn and is likely responsible for the rigidity of the structure allowing this exchangeable NH to behave like a non-exchangeable proton. This could also explain the unique NOESY correlation of Thr-NH with the NH′s of the both adjacent amino acids. Gly, Glu and HS2-NH′s showed intermediate temperature coefficient values as a result of temperature gradient suggesting a weak intra-molecular H-bonding.

2.3. Phomafungin-producing fungi

The antifungal activity of F-224,939 was detected in fermentation broths from seven of eight media tested, with a sucrose-yeast extract medium yielding the highest potency (data not shown). It was selected for scale-up fermentation. The producing fungus was determined to be *Phoma* sp. After the chemical structure was determined, five additional strains were identified as phomafungin producing fungi, based on chemical profile matching where the DAD, retention time, POS and NEG mass spectra of extracts in question were compared to the UV–LC–MS data of the authentic standard (data not shown). These extracts were tested independently in the CaFT, with profiles indistinguishable from those of the original and phomafungin (Fig. 2). These strains were collected from São Tomé and Principe, Union of Comores, Republic of South Africa, Equatorial Guinea, and New Caledonia (Supplementary data, Fig. S1). DNA barcoding with the 28S rDNA indicated that they were highly related and possibly conspecific. All were associated with soils or decaying plant material (Supplementary data, Fig. S1). The relative placement in the 28S rDNA barcode tree indicated that these fungi were members of the Pleosporales and possibly related to some species of *Massarina*.

2.4. Biological activity of phomafungin

Our results confirmed that phomafungin is the bioactive component in the original extract detected in CaFT profiling (Fig. 2). It was tested in the liquid medium for activity against a panel of fungal pathogens (Table 3). Phomafungin is active against all but one *Candida* spp. tested, at MIC 4–8 μg/ml. No activity against *C. tropicalis* was observed at 32 μg/ml. Both the filamentous *A. fumigatus* and the dermatophytic *Trichophyton mentagrophytes* are susceptible to phomafungin, at MIC of 4 and 2 μg/ml, respectively. However, in the presence of mouse/human serum, the activities against *C. albicans* and *A. fumigatus* were annihilated. It had no activity against *Staphylococcus aureus*, suggesting fungal specific growth inhibition.

Since the free acid form of phomafungin was not readily soluble in any vehicle other than DMSO, the sodium salt of phomafungin (with similar in vitro antifungal activity, data not shown) dissolved in water at 2 mg/ml was used for in vivo studies. In a mouse (DBA/2) model of disseminated Candidiasis (with *C. albicans* strain MY1055), intraperitoneal (IP) administration of phomafungin sodium salt at 50, 25, and 12.5 mg/kg (twice daily for 2 days) resulted in lethality. At lower doses (<5 mg/kg) or with PO dosing, no efficacy or lethality was observed (data not shown). Pharmacokinetic measurements indicated lack of significant exposure of phomafungin in vivo, with a normalized AUC of 2.64 μM h (in IV PK), and a clearance rate of 6.15 ml/min/kg with $t_{1/2}$ of 1.8 h (data not shown). Contrary to its strong in vivo toxicity, toxicities of phomafungin against mammalian cell lines such as, HCT116 (IC_{50} 20 μM), PC-3 (IC_{50}19 μM), GTL16 (IC_{50} 26 μM), and HEL (IC_{50} 15.5 μM), was modest. In addition, the hydrolytic linear peptide **2** displayed no antifungal activity at 32 μg/ml or in vivo efficacy against *C. albicans* MY1055. Nor was it toxic to mice at 12.5 mg/kg when administered IP, twice daily for 2 days, suggest that antifungal activity of phomafungin may be linked to its toxicity.

Phomafungin is structurally related to a group of cyclic lipodepsipeptides, including syringomycin E,[18] syringostatin,[23] syringotoxin,[23] pseudomycin A[24] and cormycin A,[25] all of which are produced by plant associated *Pseudomonas* spp. They contain a closed ring of nine (instead of eight, as in the case of phomafungin) amino-acids linked to a fatty acid hydrocarbon tail of variable length, and are important virulent factors for the phytopathogenic bacteria that may play a role in biological control of phytopathogenic fungi. Although the peptide rings are polar, cyclic lipo(depsi)peptides produced by *Pseudomonas* spp., syringomycin E, syringopeptin[26] and others, form ion channels in the host plasma membrane leading to cytolysis.[27] It was demonstrated that the effect exerted on plasma membrane by syringomycin E is Ca^{2+}-dependent.[28] Interestingly, its antifungal activity was genetically linked to sphingolipid biosynthesis in *S. cerevisiae*,[18,29] which is

Table 3
Spectrum of antifungal activity MIC-100 (MIC-80) μg/mL of phomafungin

Organism	Strain	Time of incubation (h)	Phomafungin	Caspofungin
Candida albicans	MY1055	24	4	0.125 (<0.03)
C. albicans + 50% mouse serum	MY1055	24	>32	0.25 (0.125)
C. glabrata	MY1381	24	8 (4)	0.125 (<0.03)
C. parapsilosis	ATCC22019	24	4	0.5
C. lusitaniae	MY1396	24	4	0.125 (<0.03)
C. krusei	ATCC6258	24	4	1 (0.25)
C. tropicalis	MY1012	24	>32	0.125 (<0.03)
Aspergillus fumigatus	MF5668	48	4	>32 (<0.03)
A. fumigatus + 50% human serum	MF5668	48	>32	>32 (0.06)
Trichophyton mentagrophytes	MF7004	96	2 (1)	32 (0.03)
Staphylococcus aureus	MB2865	24	>32	32

The number in parenthesis is either MIC-80 = prominent inhibition of growth for yeasts or MEC = morphological change in growth-narly hyphae microscopically for filamentous fungi *Aspergillus fumigatus and Trichophyton mentagrophytes*.

intrinsically susceptible to fluctuation in Ca^{2+}.[30] CaFT profiling indicates phomafungin is mechanistically distinguished from inhibitors of the sphingolipid biosynthesis (Fig. 2) and ionophores such as monensin, narasin, nystatin and salinomycin (data not shown). Since syringomycin E has not been tested in the CaFT, we have no direct knowledge if phomafungin is mechanistically related to it. However there are indications in the CaFT profile that the latter is genetically connected to the sphingolipid and Ca^{2+}. Four heterozygotes hypersensitive to phomafungin correspond to genes involved in sphingolipid biosynthesis: *LCB2*, *RTA2*/*RSB1*, *MIT1*/*SUR1*/*CSH1*, and *AUR1* (Fig. 2). In *S. cerevisiae*, deletion of *ScSUR2* and *ScIPT1* confers resistance to syringomycin E.[18,29] In *C. albicans*, however, heterozygous deletion of *SUR2* (*orf19.5818*) showed no preferential response to phomafungin, while that of *IPT1* (*orf19.4969*) was hypersensitive (data not shown). Furthermore, the heterozygous deletion strain for calmodulin gene (*CMD1*) displayed hypersensitivity to phomafungin. Those for a Ca^{2+}-binding protein (*FRQ1*) and a vacuolar Ca^{2+}-ATPase involved in regulating the ions (*PMC1*) were hyposensitive (Fig. 2).

It is unlikely that phomafungin and syringomycin E are mechanistically identical. The CaFT profiles of the former and the extracts of *Phoma* spp. are complex and peculiar. Although complex profiles are seen in the fitness test occasionally, biological coherence is evident in the CaFT profiles of parnafungin (an inhibitor of RNA poly(A) polymerase,[9]) and 5-fluorocytosine (affecting primarily ribosome biogenesis[8]). The lack of such biological coherence in the case of phomafungin is reminiscent of amphotericin B and toxic analogs of ergosterol.[8] CaFT profiling alone does not provide sufficient evidence for the mechanism of action for the cyclic lipodepsipeptide that we isolated. However, we speculate that phomafungin exerts its primary effect on the plasma membrane and that this activity is affected by changes in sphingolipid content and Ca^{2+} concentration.

2.5. Summary and conclusion

Cyclic lipodepsipeptides are diverse secondary metabolites produced by various organisms in terms of chemical structures and biological activities, as afforded by the variable peptide ring sizes and lipid tails. Their antiproliferative properties have been successfully exploited in antimicrobial therapeutics, for example, echinocandins (caspofungin, micafungin, and anidulafungin, inhibitors of cell wall synthesis),[31] daptomycin (targeting bacterial plasma membrane).[32] Plant/soil-associated microbes provide a rich source of secondary metabolites, whose biological activities are involved in microbe-microbe and microbe-plant interactions.[33] Based on the unique *C. albicans* fitness test profile, we isolated a cyclic lipodepsipeptide, phomafungin (**1**, Fig. 1), from a widespread tropical soil fungus, *Phoma* sp. It is structurally related to a group of bacterial cyclic lipodepsipeptides represented by syringomycin E, and is active against *Candida* spp. (with the exception of *C. tropicalis*), *T. mentagrophytes* and *A. fumigatus*. The premise of our strategy of biological dereplication using the CaFT is the association of biological activities with chemical structures. Phomafungin provides another example that substantiated such a strategy. While the compound is toxic to mice, its application in treatment of topical fungal infection has not been tested. Its precise mechanism of action remains to be determined, so does its role as virulence factor, if the producing *Phoma* sp. is phytopathogenic.

3. Experimental

All reagents were obtained from Sigma–Aldrich and were used without further purification. The NMR spectra were obtained on a Varian Inova 500 or 600 MHz spectrometers operating at 500 or 600 MHz for ^{1}H and 125 or 150 MHz for ^{13}C nuclei. The chemical shifts were referenced to DMSO-d_6 (δ_H 2.49 ppm) and (δ_C 39.5 ppm). ^{15}N chemical shifts were referenced to the lock frequency using the ^{15}N frequency ratio for NH_3 (VnmrJ2.2c).[34] Data were collected uniformly at 25 °C in 3 mm NMR tubes. A Nalorac 3 mm H{CN} indirect Z-gradient probe was used for all samples. Varian standard pulse sequences were used for all data collection. The 2D TOCSY data were collected with a 4900 Hz spin-lock field held for 80 ms, using the flopsy16 mixing scheme. Proton homonuclear correlation data were obtained with the Varian COSY or gDQF-COSY, or NOESY (mixing time 300 and 600 ms) pulse sequences. ROESY data were collected using a 4500 Hz spin-lock field applied for 200 ms. Single and multiple bond heteronuclear connectivity data were observed using the gHSQC and gHMBC pulse sequences, respectively. The gHMBC data were collected using a mixing time optimized for a 7 Hz heteronuclear coupling constant. Optical rotations were obtained on a Perkin–Elmer 241 Polarimeter; IR spectral data were obtained on a Perkin–Elmer Spectrum One spectrometer. UV spectrum was recorded on a Perkin Elmer Lambda 35 UV–vis spectrometer. High-resolution mass spectra were obtained on a Thermo Finnigan LTQ-FT using electrospray ionization using a Finnigan Ion Max source with source fragmentation on and equal to 18 V.

3.1. Fungal material

The fungal strain, F-224,939, was isolated from phenol-pasteurized soil collected in Séréhini, Grand Comore, Union of the Comoros (Supplementary data, Fig. S1). Additional strains that produced cyclic lipodepsipeptide phomafungin are listed in Fig. S1 (Supplementary data). Strains were maintained as frozen mycelium in 10% glycerol at −80 °C.

3.2. DNA sequencing and and characterization of fungal strains

Total genomic DNA was extracted from mycelia grown on YM agar. The rDNA region containing the partial sequence of 28S rDNA including the D1D2 variable domains was amplified with primers NL1 and NL4 or LROR and LR6. Sequences of 28S rDNA were used to generate a neighbor-joining tree (Supplementary data, Fig. S1) that demonstrated the close relationships among the phomafungin producing strains. To achieve further phylogenetic resolution, the same genomic DNA samples were used to generate sequences of the intertranscribed spacer regions and 5.8S gene of the rDNA (ITS) which also indicated that *Massarina* was the most closely related genus.

PCR reactions were performed following the standard procedures (5 min at 93° followed by 40 cycles of 30 s at 93 °C, 30 s at 53 °C and 2 min at 72 °C) with Taq DNA polymerase (Q-bio-Gene) as recommended by the manufacturer. The amplification products (0.10 μg/ml) were sequenced using the Bigdye Terminators version 1.1 (Perkin Elmer, Norwalk, Connecticut, USA) following the manufacturer's recommendations. For all the amplification products, each strand was sequenced with the same primers used for the initial amplification. Partial sequences were assembled using Genestudio software (Genestudio, Inc.), and consensus sequences were aligned by the same software. Neighbor-joining analyses were used to approximate phylogenetic relationships among strains.

3.3. Fermentations in nutritional arrays and scale up for isolation

Our screening strategy relied on high throughput generation of 1 ml-scale extracts of organisms grown under varied fermentation parameters followed by assay for antibiosis caused by cell-penetrable molecules against *C. albicans* and *S. aureus*. Organism-and-med-

ium combinations yielding extracts with a minimum potency and activity spectrum were scaled up to provide larger fermentations suitable for profiling in the CaFT, further processing for an extract library, and for chemical fractionation, if needed. The strategy and protocols for fermentation of fungi on nutritional microarrays has been described previously.[5] Each week, 160–240 fungal strains were selected for fermentations. These fungi were grown 2–3 weeks in 60-mm Petri dishes containing YM agar (Fluka or Difco malt extract 10 g, Difco yeast extract 2 g, agar 20 g, distilled H_2O 1000 mL). Three to four mycelial discs were cut from each 60-mm plate. Mycelia discs were crushed in the bottom of tubes (25 × 150 mm) containing 8 mL of SMYA medium (Difco neopeptone 10 g, maltose 40 g, Difco yeast extract 10 g, agar 4 g, distilled H_2O 1000 mL) and two cover glasses (22 mm^2). Tubes were agitated on an orbital shaker (200 rev min^{-1}, 5 cm throw), and rotation of the cover glasses continually sheared hyphae and mycelial disc fragments to produce homogenous hyphal suspensions. Tubes were agitated 4–6 d at 22 °C. Hyphal suspensions from these tubes were transferred to master inoculum plates. Master plates of fungal inoculum were used to inoculate 8-media nutritional arrays in a ten-column × eight-row pattern.[5] Nutritional arrays were grown statically 21 d at 22 °C.

The detection of antifungal activity from strain F-224,939 originated from an 1 ml fermentation in the medium YES (sucrose 150 g; yeast extract (Becton Dickinson) 20 g; $MgSO_4{\cdot}7H_2O$ 0.5 g; $ZnSO_4{\cdot}7H_2O$ 0.01 mg; $CuSO_4{\cdot}5H_2O$ 0.005 mg, distilled H_2O 10,000 mL). It was scaled up to 1 L by growing F-224,939 in 500 ml flasks with 150 mL of liquid YES agitated at 220 rpm, 22 °C for 22 d. The liquid fermentations were extracted with an equal volume of acetone and pooled. A 4 ml aliquot was frozen and tested for CaFT and remaining extract was used for isolation of active metabolites.

3.4. Extraction and Isolation of phomafungin (1)

A 0.5 L fermentation broth (pH 7) was extracted with 0.5 L of acetone and chromatographed on a 50 mL medium grade Amberchrome reversed-phase column and eluted with a 100 min 5–100% aqueous MeOH gradient. Activity eluted in the 90–100% MeOH was concentrated and lyophilized to yield 200 mg solid material. An aliquot of 130 mg from the Amberchrome active fraction was subjected to successive liquid–liquid partitioning using water and hexane, dichloromethane, ethyl acetate, and methyl ethyl ketone (MEK). The active compound was concentrated in the MEK extract. The latter extract was concentrated and lyophilized to yield 79 mg pale yellow solid material. Finally, a 25 mg aliquot of the solid material was chromatographed on a Zorbax RX C_8 (21.2 × 250 mm) column eluting at a flow rate of 12 ml/min with a 37 min gradient of 10 to 95% aqueous CH_3CN containing 0.1% TFA. Fractions eluting at 26–27 min were concentrated, lyophilized to yield 15 mg (156 mg/l) of phomafungin (**1**) as an amorphous powder. $[\alpha]_D^{23}$ = +57.1 (*c*, 0.42, sodium salt in water); UV (CH_3CN) λ_{max} end absorption; IR (ZnSe) ν_{max} 3310, 2926, 1624, 1536 cm^{-1}; HRESTFTMS (*m/z*)1029.5606 (calcd for $C_{46}H_{79}N_9O_{17}$, 1029.5594), ^1H and ^{13}C NMR data, see Table 1.

3.5. Hydrolysis of phomafungin

To a suspension of phomafungin (20 mg) in 7 ml water was added 5 ml of 0.01 M NaOH at room temperature and the solution was stirred for 1 h. The reaction mixture was charged on a small column of Amberchrome and washed with water and the sodium salt of the acyclic peptide was eluted with MeOH which was concentrated and lyophilized to yield 18 mg of open form of the peptide **2**, as an amorphous powder. HRESTFTMS (*m/z*) 1048.5768 (calcd for $C_{46}H_{81}N_9O_{18}$+H, 1047.5778), ^1H NMR (600 MHz) DMSO-d_6 δ 8.58 (1H, br s), 8.49 (1H, br s), 8.26 (3H, br s), 8.17 (1H, d, *J* = 7.2 Hz), 7.88 (1H, br s), 7.64 (1H, br d, *J* = 7.2 Hz), 7.43 (1H, br s), 6.80 (1H, br s), 4.42 (1H, br q, *J* = 7 Hz), 4.25 (2H, m), 4.19 (2H, m), 3.97 (1H, t, *J* = 6.6 Hz), 3.85 (1H, q, *J* = 6.6 Hz), 3.80 (1H, dd, *J* = 17.4, 6.6 Hz), 3.76 (1H, t, *J* = 6.6 Hz), 3.67 (1H, m), 3.64 (2H, m), 3.55 (1H, dd, *J* = 11.4, 4.2 Hz), 3.52 (1H, m), 3.40 (1H, m), 3.36 (1H, m), 2.26 (1H, m), 2.08–2.14 (4H, m), 1.77–1.91 (4H, m), 1.59–1.70 (2H, m), 1.27–1.42 (2H, m), 1.22 (23H, m), 1.18 (3H, d, *J* = 6.6 Hz), 0.98 (3H, d, *J* = 6.0 Hz), 0.83 (3H, t, *J* = 7.2 Hz), 0.77 (3H, d, *J* = 6.6 Hz).

3.6. The *C. albicans* fitness test

The *C. albicans* fitness test was performed as described.[8] Briefly, 5-ml cultures of the pool (at the initial OD_{600} of 0.025) were treated with antifungal actives (compounds and extracts) at multiple concentrations together with the mock treatment. The active inhibitory concentration of each culture was determined after 15 h at 30 °C. Those with desirable ICs were retained, and diluted to OD_{600} 0.05 with medium containing the antifungal active at the original concentrations. After another 23 h of growth, cell pellets were collected, and total genomic DNA prepared. DNA samples of the treated and the mock cultures were PCR amplified using common primers that flank the strain-specific barcodes, and labeled. Mixtures of labeled barcodes were hybridized against DNA microarrays. The relative responses (hyper- and hypo-sensitivities) of each strain in the treated culture was appraised using an error-modeling statistic framework that involves a set of ~50 reference compounds, and expressed by normalized *z*-scores of both up- and down-stream barcodes (see Ref. 8 for details). For each strain, the *z*-score with higher absolute value is selected to compile the final list. Cluster 3.0 was used to analyze multiple fitness test experiments, the result of which was displayed with TreeView. Both are available at http://bonsai.ims.u-tokyo.ac.jp/~mdehoon/software/cluster/software.htm.

3.7. Antifungal assay

The MIC (minimum inhibitory concentration) against each of the strains was determined as previously described.[35] Briefly, cells were inoculated at 10^5 colony-forming units/ml followed by incubation at 37 °C with a 2-fold serial dilution of compound in the growth medium for 20 h. MIC is defined as the lowest concentration of an antibiotic inhibiting visible growth.

3.8. In vivo assay

Mice were infected i.v. (lateral tail veins) with *C. albicans* MY1055 at 2.51 × 10^4 CFU/mouse. Five DBA/2 mice in each group were treated with sodium salt of phomafungin was formulated in water and treated at 50, 25, 12.5, 5, 2.5 mg/kg twice daily by IP administration. Mice were observed for mortality and general health for 4 days after challenge, after which they were euthanized, with both kidneys aseptically removed, placed in sterile Whirl-Pak bags, weighed and then homogenized in 5 ml of sterile saline. Kidney homogenates were then serially 10-fold diluted in sterile saline and plated on SDA. Plates were incubated at 35 °C and counted after 30–48 h. Colony forming units (CFU) per gram of kidney were determined and counts from treatment groups compared to counts from sham-treated controls using a paired two tailed t-Test (Excel).

Acknowledgments

We would like to thank M. Arocho, K. Calati, K. Ferguson and J. Occi for the preliminary isolation and assay support.

Supplementary data

^{1}H and ^{13}C NMR and CaFT profile of phomafungin (1), Fig. S1 neighbor-joining analysis of 28S sequences. Supplementary data associated with this article can be found, in the online version, at doi:10.1016/j.bmc.2008.12.009.

References and notes

1. Hof, H. *Eur. J. Clin. Microbiol. Infect. Dis.* **2008**, *27*, 327.
2. Gallis, H. A.; Drew, R. H.; Pickard, W. W. *Rev. Infect. Dis.* **1990**, *12*, 308.
3. Zonios, D. I.; Bennett, J. E. *Sem. Respir. Crit. Care Med.* **2008**, *29*, 198.
4. Georgopapadakou, N. H. *Expert Opin. Invest. Drugs* **2001**, *10*, 269.
5. Bills, G. F.; Platas, G.; Fillola, A.; Jimenez, M. R.; Collado, J.; Vicente, F.; Martin, J.; Gonzalez, A.; Bur-Zimmermann, J.; Tormo, J. R.; Pelaez, F. *J. Appl. Microbiol.* **2008**, *104*, 1644.
6. Haselbeck, R.; Wall, D.; Jiang, B.; Ketela, T.; Zyskind, J.; Bussey, H.; Foulkes, J. G.; Roemer, T. *Curr. Pharm. Des.* **2002**, *8*, 1155.
7. Roemer, T.; Jiang, B.; Davison, J.; Ketela, T.; Veillette, K.; Breton, A.; Tandia, F.; Linteau, A.; Sillaots, S.; Marta, C.; Martel, N.; Veronneau, S.; Lemieux, S.; Kauffman, S.; Becker, J.; Storms, R.; Boone, C.; Bussey, H. *Mol. Microbiol.* **2003**, *50*, 167.
8. Xu, D.; Jiang, B.; Ketela, T.; Lemieux, S.; Veillette, K.; Martel, N.; Davison, J.; Sillaots, S.; Trosok, S.; Bachewich, C.; Bussey, H.; Youngman, P.; Roemer, T. *PLoS Pathog.* **2007**, *3*, e92.
9. Jiang, B.; Xu, D.; Allocco, J.; Parish, C.; Davison, J.; Veillette, K.; Sillaots, S.; Hu, W.; Rodriguez-Suarez, R.; Trosok, S.; Zhang, L.; Li, Y.; Rahkhoodaee, F.; Ransom, T.; Martel, N.; Wang, H.; Gauvin, D.; Wiltsie, J.; Wisniewski, D.; Salowe, S.; Kahn, J. N.; Hsu, M. J.; Giacobbe, R.; Abruzzo, G.; Flattery, A.; Gill, C.; Youngman, P.; Wilson, K.; Bills, G.; Platas, G.; Pelaez, F.; Diez, M. T.; Kauffman, S.; Becker, J.; Harris, G.; Liberator, P.; Roemer, T. *Chem. Biol.* **2008**, *15*, 363.
10. Parish, C. A.; Smith, S. K.; Calati, K.; Zink, D.; Wilson, K.; Roemer, T.; Jiang, B.; Xu, D.; Bills, G.; Platas, G.; Pelaez, F.; Diez, M. T.; Tsou, N.; McKeown, A. E.; Ball, R. G.; Powles, M. A.; Yeung, L.; Liberator, P.; Harris, G. *J. Am. Chem. Soc.* **2008**, *130*, 7060.
11. Kluepfel, D.; Bagli, J.; Baker, H.; Charest, M. P.; Kudelski, A. *J. Antibiot. (Tokyo)* **1972**, *25*, 109.
12. Ikai, K.; Takesako, K.; Shiomi, K.; Moriguchi, M.; Umeda, Y.; Yamamoto, J.; Kato, I.; Naganawa, H. *J. Antibiot. (Tokyo)* **1991**, *44*, 925.
13. Nagiec, M. M.; Nagiec, E. E.; Baltisberger, J. A.; Wells, G. B.; Lester, R. L.; Dickson, R. C. *J. Biol. Chem.* **1997**, *272*, 9809.
14. Mandala, S. M.; Thornton, R. A.; Milligan, J.; Rosenbach, M.; Garcia-Calvo, M.; Bull, H. G.; Harris, G.; Abruzzo, G. K.; Flattery, A. M.; Gill, C. J.; Bartizal, K.; Dreikorn, S.; Kurtz, M. B. *J. Biol. Chem.* **1998**, *273*, 14942.
15. Mandala, S. M.; Harris, G. H. *Methods Enzymol.* **2000**, *311*, 335.
16. Vicente, M. F.; Basilio, A.; Cabello, A.; Pelaez, F. *Clin. Microbiol. Infect.* **2003**, *9*, 15.
17. Ikai, K.; Shiomi, K.; Takesako, K.; Mizutani, S.; Yamamoto, J.; Ogawa, Y.; Ueno, M.; Kato, I. *J. Antibiot. (Tokyo)* **1991**, *44*, 1187.
18. Grilley, M. M.; Stock, S. D.; Dickson, R. C.; Lester, R. L.; Takemoto, J. Y. *J. Biol. Chem.* **1998**, *273*, 11062.
19. Ohnishi, M.; Urry, D. W. *Biochem. Biophys. Res. Commun.* **1969**, *36*, 194.
20. Gellman, S. H.; Dado, G. P.; Liang, G. B.; Adams, B. R. *J. Am. Chem. Soc.* **1991**, *113*, 1164.
21. Andersen, N. H.; Neidigh, J. W.; Harris, S. M.; Lee, G. M.; Liu, Z.; Tong, H. *J. Am. Chem. Soc.* **1997**, *119*, 8547.
22. Singh, S. B.; Zink, D. L.; Liesch, J. M.; Mosley, R. T.; Dombrowski, A. W.; Bills, G. F.; Darkin-Rattray, S. J.; Schmatz, D. M.; Goetz, M. A. *J. Org. Chem.* **2002**, *67*, 815.
23. Fukuchi, N.; Isogai, A.; Nakayama, J.; Takayama, S.; Yamashita, S.; Suyama, K.; Takemoto, J. Y.; Suzuki, A. *J. Chem. Soc., Perkin Trans. 1* **1992**, 1149.
24. Di Giorgio, D.; Camoni, L.; Marchiafava, C.; Ballio, A. *Phytochemistry* **1997**, *45*, 1385.
25. Scaloni, A.; Dalla Serra, M.; Amodeo, P.; Mannina, L.; Vitale, R. M.; Segre, A. L.; Cruciani, O.; Lodovichetti, F.; Greco, M. L.; Fiore, A.; Gallo, M.; D'Ambrosio, C.; Coraiola, M.; Menestrina, G.; Graniti, A.; Fogliano, V. *Biochem. J.* **2004**, *384*, 25.
26. Szabo, Z.; Budai, M.; Blasko, K.; Grof, P. *Biochim. Biophys. Acta* **2004**, *1660*, 118.
27. Raaijmakers, J. M.; de Bruijn, I.; de Kock, M. J. *Mol. Plant Microbe Interact.* **2006**, *19*, 699.
28. Bidwai, A. P.; Takemoto, J. Y. *Proc. Natl. Acad. Sci. U.S.A.* **1987**, *84*, 6755.
29. Stock, S. D.; Hama, H.; Radding, J. A.; Young, D. A.; Takemoto, J. Y. *Antimicrob. Agents Chemother.* **2000**, *44*, 1174.
30. Dickson, R. C.; Sumanasekera, C.; Lester, R. L. *Prog. Lipid Res.* **2006**, *45*, 447.
31. Cappelletty, D.; Eiselstein-McKitrick, K. *Pharmacotherapy* **2007**, *27*, 369.
32. Baltz, R. H.; Miao, V.; Wrigley, S. K. *Nat. Prod. Rep.* **2005**, *22*, 717.
33. Gunatilaka, A. A. *J. Nat. Prod.* **2006**, *69*, 509.
34. Harris, R. K.; Becker, E. D.; Cabral de Menezes, S. M.; Goodfellow, R.; Granger, P. *Pure Appl. Chem.* **2001**, *73*, 1795.
35. Bartizal, K.; Scott, T.; Abruzzo, G.; Gill, C.; Pacholok, C.; Lynch, L.; Kropp, H. *Antimicrob. Agents Chemother.* **1995**, *39*, 1070.
36. Eisen, M. B.; Spellman, P. T.; Brown, P. O.; Botstein, D. *Proc. Natl. Acad. Sci. U.S.A.* **1998**, *95*, 14863.